ELSEVIER

Journal of Nuclear Materials 313–316 (2003) 636–640

journal of nuclear materials

www.elsevier.com/locate/jnucmat

D^+, He^+ and H^+ sputtering of solid and liquid phase tin

M.D. Coventry *, J.P. Allain, D.N. Ruzic

Nuclear, Plasma, and Radiological Engineering, University of Illinois, Urbana-Champaign, 103 S. Goodwin Avenue, Urbana, IL 61801, USA

Abstract

Absolute sputtering yields of Sn in the solid and liquid phases for incident H^+, D^+, and He^+ ions with energies of 300 to 1000 eV were determined via a series of experiments using the ion-surface interaction experiment (IIAX), a facility designed to measure such ion-surface interactions. IIAX incorporates an ion source with an array of ion beam filters and optics to bring a near mono-energetic beam of ions to the target, in this case at 45° to the surface normal. A pair of quartz crystal microbalances record the amount of mass collected from both sputtering and evaporation from the target. VFTRIM-3D modeling results of tin sputtering best fit the experimental data when the bulk of pure tin was modeled with 60% SnO coverage in the top three monolayers most likely indicating the presence of a very thin oxide layer during experimentation.

Keywords: Plasma-material interaction; Tin sputtering; Ion-beam irradiation; Liquid-metal sputtering; Divertor material

1. Introduction

The level of success of next step tokamak devices is dependent upon the development of a suitable surface material for plasma facing components. The divertor materials in particular must withstand an increased frequency of transient thermal power loads on the order of a few to tens of MW/m^2 [1] due to the off-normal plasma events as well as compatible with the increased duty cycles of these next-step machines. The material must have manageable sputtering and evaporation rates to minimize impurities entering the plasma and suitable thermal, chemical, and nuclear properties. The use of flowing liquid metals has been under recent investigation [2,3] because of their capability to handle these high thermal loads and their self-healing nature – i.e. any physical damage is repaired quickly by the flowing liquid metal. The principal liquid metal candidates are Li, Sn–Li, and Sn.

The sputtering properties of both solid and liquid lithium [4,5] and 0.8 Sn–Li [6] have been previously examined at the ion-surface interaction experiment (IIAX) facility. While lithium has the distinct advantage of having a lower-Z thus allowing a two to three orders of magnitude increase (based on Z^2 to Z^3 scaling) in the substitutional impurity within the plasma over tin, tin has the advantage of having five or more orders-of-magnitude lower vapor pressure (Fig. 1 is based on a theoretical model [7] for the pure metal case and an empirical fit [8] for the tin–lithium case); also, tin's surface tension is higher than that of lithium roughly by a factor of 1.7 at 300 °C [9] improving the stability of the liquid wall. Previous work on tin sputtering is limited to only measurements of tin-oxide sputtering [10,11] and self-sputtering of tin [12]. Therefore, the main motivation of this work is to measure the sputtering yield of tin in the solid and liquid states from typical impurity/incident ions in a fusion machine environment and determine its viability as future plasma-facing material.

2. Experiment design and set-up

The IIAX is specifically tailored to measure the absolute sputtering yields of both solid and liquid targets

* Corresponding author. Fax: +1-217 333 2906.
E-mail address: coventry@uiuc.edu (M.D. Coventry).

0022-3115/03/$ - see front matter
PII: S0022-3115(02)01369-7

from low-energy ion beam irradiation. As shown in Fig. 2, IIAX consists of an ion gun chamber and a target chamber containing the target and diagnostics, both of which routinely reach base pressures of 10^{-9} Torr. The ion gun chamber is differentially pumped to minimize the pressure in the main chamber and reduce ion-neutral scattering.

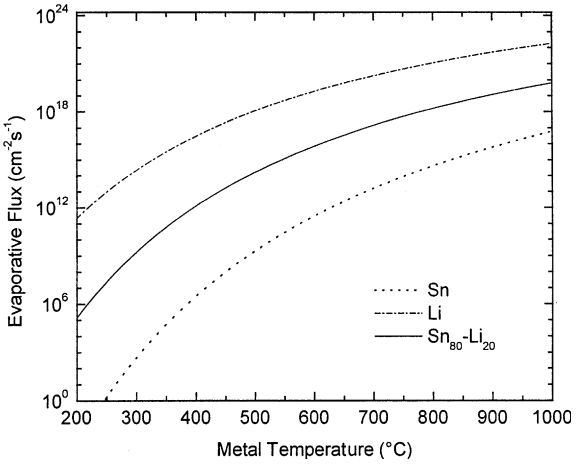

Fig. 1. Evaporative fluxes of lithium, 0.8 Sn–Li, and tin. The pure metal curves were obtained using a theoretical model [7] specifically for liquid metals and the alloy plot is from an empirical fit [8] to experimental data.

The ion gun employed uses electron-impact ionization for gaseous species and thermionic emission for powdered solids. The ions are accelerated and pass through an $E \times B$ filter to remove all ion species except those with the desired charge-to-mass ratio and velocity. Once the ions enter the target chamber, they pass through a deceleration region (only active for low-energy beams) and finally pass through a neutral filter to remove the beam's neutral component before striking the target.

The target is situated in the center of the main chamber currently with its surface normal 45° off of the beam axis to best simulate the average impact angle of ions striking a tokamak divertor surface [13]. A boron nitride (BN) cup houses the target and a UHV heater that is used to heat the sample to roughly 10° above its 230 °C melting temperature for the liquid runs; this temperature is monitored by a thermocouple on the exterior of the BN target retainer cap and is calibrated to the temperature at the target. The target is a vertical surface with a stainless steel retention shield in front to minimize exposed surface area prone to flow initiation during the liquid series of experiments.

700 eV He^+ beams were used to sputter-clean the top layer of the target. A necessary ion fluence of 10^{17} ions/

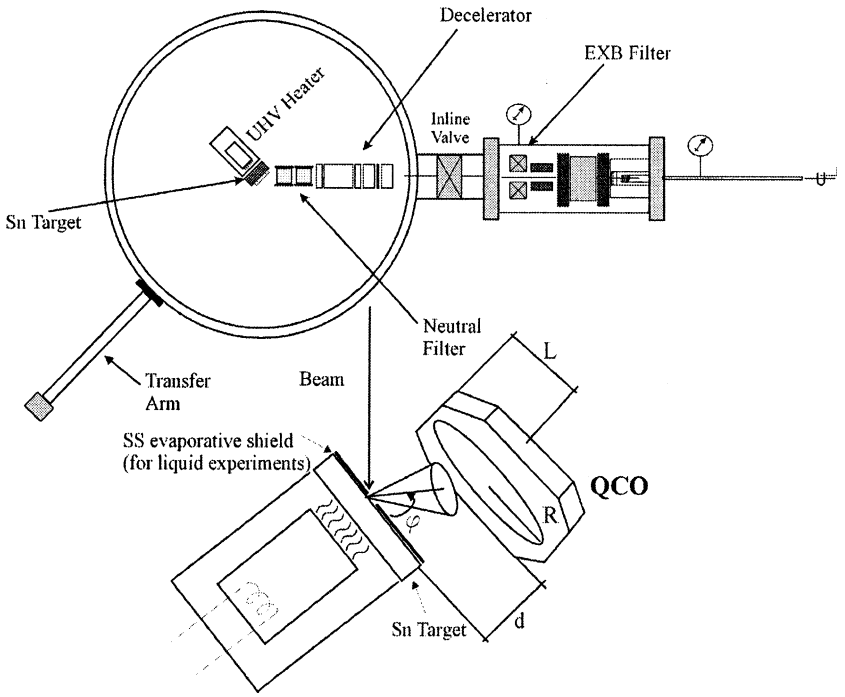

Fig. 2. Schematic of the IIAX at the University of Illinois at Urbana-Champaign. The ion gun chamber is located on the right and on the left the main chamber is where the target is located. The close-up diagram shows the position of the tin target with respect to the quartz crystal oscillator (QCO). The specific geometry of the QCO/target system is taken into account during data analysis.

cm^2 was calculated via the estimated oxidation thickness on the order of 30 Å based on reported measurements [14] and the oxygen partial sputtering yield from a TRIM simulation [15].

A quartz–crystal microbalance (QCM) is placed near the target and measures the mass of material deposited on it due to target erosion. A second crystal is located outside of the solid angle of the sputtered material to account for the environmental, non-ion beam induced effects. Details of this technique can be found in previous work [4]. Data recorded during irradiation includes direct measurement of the ion beam current, the frequencies of the crystals, the temperature BN cap, and partial pressures of select gases all as a function of time.

3. Data analysis

The QCM measures the amount of mass deposited on the crystal through measuring the change in crystal oscillation frequency relative to its fundamental frequency, as the fractional change in frequency is directly proportional to the fractional change in mass when the deposited film is much thinner than the crystal. The sticking and reflection coefficients are calculated from simulation runs using VFTRIM-3D [16], a Monte Carlo collision model that uses a fractal algorithm to simulate surface roughness. In this case, it is assumed that as tin is deposited onto the crystal, it is oxidized by the background partial pressure of oxygen (on the order of 10^{-18} Torr), which increases the mass measured.

Corrections are also made to account for the fraction of material measured to that sputtered based on the target-crystal geometry and the sputtered particle distribution. Also determined is the total crystal mass loss due to sputtering of previously deposited material by both ions reflected from the target and by neutrals sputtered from the target. Uncertainty calculations contain elements of all of these adjustments as well as the experimental uncertainty and are usually around 40%. The overall sputtering yield is determined by the fractional change in oscillator frequency $\Delta f/f$ divided by the product of the ion dose D, sticking coefficient of tin onto the gold crystal S^{QCO}, the fraction of sputtered material that reaches the crystal Ω, the mass of the assumed final species (in this case m_{SnO}), and the amount of material resputtered from the crystal due to reflected ions $(1 + Y^{\mathrm{QCO}}R^{\mathrm{QCO}})$ and is given by

$$Y_{\mathrm{sp}} = \frac{1}{DS^{\mathrm{QCO}}\Omega m_{\mathrm{SnO}}}\frac{\Delta f}{f}M_{\mathrm{crystal}}\left(1 + Y_j^{\mathrm{QCO}}R_j^{\mathrm{QCO}}\right). \quad (1)$$

4. Computational modeling

Computational modeling for tin sputtering is done with the VFTRIM-3D model [16], based on TRIM-SP and modified to simulate atomic-scale surface roughness. Surface roughness is modeled using a fractal dimension of 2.05. VFTRIM-3D has been shown to successfully predict the sputtering and reflection coefficients of various particle/target systems [4,6,16] including that for 0.8 Sn–Li in the solid and liquid state [6].

In VFTRIM-3D the surface binding energy (SBE) applies the heat of sublimation of the material as a key parameter at these low energies. This version of VFTRIM-3D uses an equipartition between the local Oen–Robinson inelastic energy loss model and a non-local Lindhard–Sharff inelastic energy loss model. For pure tin and tin oxide sputtering, the model in VFTRIM-3D used SBEs of 3.12 and 0.35 eV [10] respectively. The incident particle energies were varied from 25 eV up to 3 keV at 45° incidence to normal with primary interest in those at energies used in experiment.

In order to approximate the amount of oxide present on the surface, both concentration and thickness were varied. The best fit to the experimental data resulted from a three-monolayer surface with 60% coverage of SnO resulting in a SBE of 1.46 eV calculated from approximating the binding energy as the weighted average of binding energies of Sn and SnO.

5. Results and discussion

Table 1 summarizes measured sputtering yields of tin in the solid and liquid phase due to bombardment by H^+, D^+ and He^+ ions with energies between 300 and 1000 eV at 45° incidence. Fig. 3 compares computational results from both models considered by VFTRIM-3D to the experimental results. Helium bombardment of tin in the liquid phase at just above the melting point the

Table 1
A summary of the sputtering yields recorded during this study. Some oxidation of the surfaces is likely

Incident ion energy (eV)	D^+ on solid Sn	H^+ on solid Sn	He^+ on solid Sn	He^+ on liquid Sn (240 °C)
300	0.038 ± 0.013	0.009 ± 0.003	–	–
500	0.055 ± 0.017	0.012 ± 0.005	0.219 ± 0.054	–
700	0.072 ± 0.022	0.018 ± 0.008	0.357 ± 0.088	0.443 ± 0.144
1000	0.107 ± 0.042	0.040 ± 0.020	0.423 ± 0.136	0.504 ± 0.167

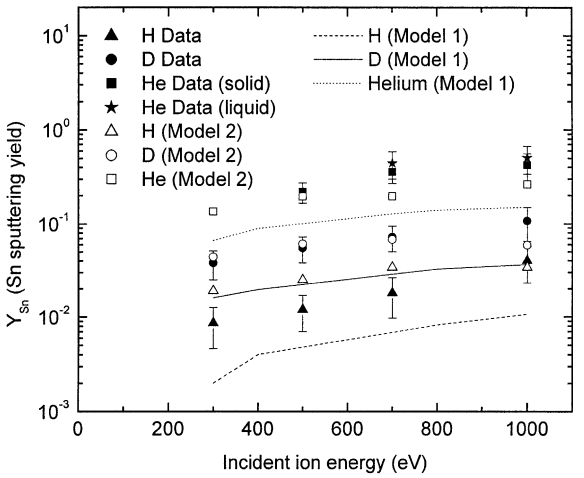

Fig. 3. IIAX data on solid and liquid tin compared to results using VFTRIM-3D assuming pure tin (model 1) and tin with 60% SnO coverage on the first two monolayers. Data and simulations are for 45° incidence.

sputtering yield lies within the experimental error bars of the solid tin data.

Helium, deuterium and hydrogen bombardment all show a linearly increasing yield for energies ranging from 100 to 1000 eV at 45° incidence. VFTRIM-3D modeling shows a sputtering threshold for helium, deuterium, and hydrogen bombardment of about 50, 100, and 120 eV respectively.

5.1. Sputtering from tin in the solid state

The sputtering yields recorded here are higher than predicted by VFTRIM-3D modeling a pure tin target. However, assuming a moderate level of oxidation on the surface, VFTRIM-3D predicts the experimental data quite well possibly indicating the presence of an oxide layer on the sample. The measured yields for tin are quite large as the incident particle energy is increased above 300 eV. This model is consistent with work by Kelly [11] that has shown sputtering from pure tin(IV)-oxide can lead to sputtering yields much greater than those predicted for a pure tin target while typically metal oxides have a reduced sputtering coefficient in comparison to their pure metal counterparts. While a number of metallic oxides have been found to have abnormally high sputtering coefficients [11,17], tin(IV)-oxide has the highest sputtering coefficient known for any *metallic* oxide and its yield increases with temperature [10]. Although those studies were done for 10 keV bombardment of Kr^+ on tin-oxide, other work reported in the same paper with 300 eV He^+ on Ta_2O_5 shows very large sputtering yields compared to bombardment with heavier incident particles and higher particle energies. The enhancement is primarily due to surface oxides causing an effective decrease of the SBE [11,18]. It is believed that the minimal surface coverage of oxygen accumulated in vacuo has caused a non-negligible amount of oxide to form and enhance sputtering from tin in the solid state.

5.2. Sputtering from tin in the liquid state

Sputtering of liquid-phase tin is indistinguishable from sputtering of tin in the solid phase at temperatures just above the melting point. This is consistent with measured sputtering yields from other liquid metals such as Li [5]. Tin-oxide sputtering does show a modest increase with target temperature. However, the yield only doubles when the temperatures of the oxide are of the order of 600 °C. For tin even some amount of oxide on the surface is not expected to dramatically change the sputtering yield when heating it just above the melting point. Future work will study the temperature dependence of tin sputtering for a variety of incident particle species and energies. In addition, if liquid tin were to be used as a plasma-facing surface, flowing liquid tin could address the negative effect of oxide coverage on tin sputtering, as the surface would be continually replenished.

5.3. Tin self-sputtering

Self-sputtering at the plasma boundary in fusion devices will occur for impurities, which have been injected towards the plasma are ionized and eventually return to strike solid surfaces at the wall or divertor regions. The momentum transfer between like-masses is extremely effective and thus particularly damaging to the

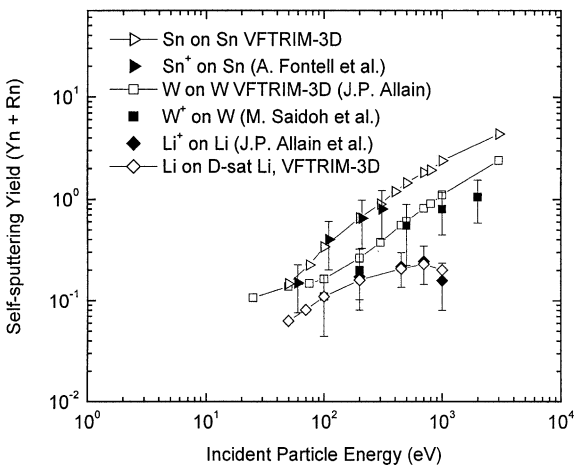

Fig. 4. Self-sputtering experimental and simulation yields (total = reflection + sputtering for VFTRIM-3D simulations) of tin, tungsten and lithium at 45° incidence. All data are for solid phase at room temperature.

surface. Therefore, determining the magnitude of tin self-sputtering is important.

There are two components in self-sputtering that must be considered. One is the erosion component due to physical sputtering, and the other is reflection of the incident particle into the plasma. Since both sources cannot be distinguished from each other, except their average particle energy, these sources must be added to obtain the total amount of particles injected into the plasma. Fig. 4 shows measurements and modeling of the self-sputtering yield (sputtering + reflection) for the cases of tin [12], lithium, and tungsten [19] at 45° incidence. Lithium and tungsten are shown for comparison and reflection coefficients are calculated using the TRIM-SP code. The self-sputtering yield of tin shows relatively large yields for energies above 100 eV with a self-sputtering threshold of about 10–20 eV.

6. Conclusions

The sputtering yield of solid-phase tin from bombardment by H^+, D^+ and He^+ at 45° incidence has been measured. The sputtering yield for liquid-phase tin from He^+ bombardment has also been measured just above the melting point of tin at 240 °C.

Results show relatively large yields from both the solid and liquid state for incident particle energies ranging from 300 to 1000 eV probably indicating the presence of a thin layer of oxygen atoms roughly three-monolayers thick, which, for the case of tin, reduces the SBE, thus enhancing the sputtering yield. These results are consistent from those of previous metallic oxide studies [10].

The use of tin as a future plasma-facing surface looks promising if reionized Sn ion energies do not exceed approximately 150 eV. Limits on impurity levels from tin erosion due to self-sputtering may be problematic if confinement conditions lead to high edge temperatures and consequently high incident particle energies. Hydrogen and helium sputtering of tin is quite low. The application of tin in the liquid phase also looks promising from an erosion standpoint if the incident particle energy is kept low. In addition, free-surface flowing tin would help contend with monolayer oxygen formation and consequently reduce the enhanced erosion measured in tin. With its relatively low vapor pressure and attractive thermophysical properties, flowing liquid tin may prove to be a viable candidate for plasma-facing material.

Acknowledgements

The authors would like to acknowledge helpful discussions with J.N. Brooks and R. Bastasz. Acknowledgement is also made to the DOE/ALPS program for financial support of this work through contract DOE DEFG 0299ER54515.

References

[1] G. Federici, C.H. Skinner, J.N. Brooks, et al., Nucl. Fusion 41 (12) (2001) 1751.
[2] R.F. Mattas et al., Fusion Eng. Des. 49&50 (2000) 127.
[3] A. Hassanein, J. Nucl. Mater. 302 (2002) 41.
[4] J.P. Allain, D.N. Ruzic, Nucl. Fusion 42 (2002) 202.
[5] J.P. Allain, D.N. Ruzic, M.R. Hendricks, J. Nucl. Mater. 290–293 (2001) 180.
[6] J.P. Allain, D.N. Ruzic, M.R. Hendricks, J. Nucl. Mater. 290–293 (2001) 33.
[7] Y. Waseda, S. Ueno, K.T. Jacob, J. Mater. Sci. Lett. 8 (1989) 857.
[8] M.A. Abdou, A. Ying, N.B. Morley et al., APEX Interim Report Report No. UCLA-ENG-99-206, 1999.
[9] S. Sharafat, N. Ghoniem, APEX Study Report No. UCLA-UCMEP-00-31, 2000.
[10] R. Kelly, E. Giani, Nucl. Instrum. and Meth. 209&210 (1983) 531.
[11] R. Kelly, N.Q. Lam, Radiat. Eff. 19 (1) (1973) 39.
[12] A. Fontell, E. Arminen, Can. J. Phys. 47 (1969) 2405.
[13] J.N. Brooks, Phys. Fluids B-Plasma Phys. 2 (8) (1990) 1858.
[14] G.B. Hoflund, G.R. Corallo, Phys. Rev. B 46 (11) (1992) 7110.
[15] J.P. Biersack, W. Eckstein, J. Appl. Phys. A 34 (1984) 73.
[16] D.N. Ruzic, Nucl. Instrum. and Meth. B 47 (1990) 118.
[17] N.Q. Lam, R. Kelly, Can. J. Phys. 48 (1970) 137.
[18] H.M. Naguib, R. Kelly, Radiat. Eff. 25 (1975) 1.
[19] M. Saidoh, K. Sone, Jpn. J. Appl. Phys. 22 (1983) 257.